

# Restrictions on the Three-Class Ideal Observer's Decision Boundary Lines

Darrin C. Edwards\* and Charles E. Metz

**Abstract**—We are attempting to develop expressions for the coordinates of points on the three-class ideal observer's receiver operating characteristic (ROC) hypersurface as functions of the set of decision criteria used by the ideal observer. This is considerably more difficult than in the two-class classification task, because the conditional probabilities in question are not simply related to the cumulative distribution functions of the decision variables, and because the slopes and intercepts of the decision boundary lines are not independent; given the locations of two of the lines, the location of the third will be constrained depending on the other two. In the present work we attempt to characterize those constraining relationships among the three-class ideal observer's decision boundary lines. As a result, we show that the relationship between the decision criteria and the misclassification probabilities is not one-to-one, as it is for the two-class ideal observer.

**Index Terms**—ROC analysis, ideal observers, three-class classification

## I. INTRODUCTION

RECEIVER operating characteristic (ROC) analysis is the accepted methodology for analyzing the performance of a two-class classifier [1], in particular for medical decision-making tasks in which a patient is diagnosed as having or not having a particular condition based on features of a medical image [2]. In judging the performance of an observer measured *via* ROC analysis, the standard for comparison is the so-called ideal observer, that observer which outperforms any other possible observer given the statistical variability of the observational data being classified [1], [3]. Although the general form of the ideal observer in a classification task with three or more classes has been known for some time [3], the considerable complexities inherent to this model compared to the two-class classification task have hampered the development of extensions of ROC analysis which are both fully general and practically useful. (Several researchers have recently proposed restricted observer models or restricted evaluation methods [4]–[7].)

Despite these difficulties, research continues in this area because the advantages to be gained from a three-class classifier and appropriate evaluation methodology are considerable. In our own case, we seek to combine existing computer-aided diagnosis (CAD) schemes for detecting [8]–[12] mammographic mass lesions and classifying [13]–[17] them as malignant or

benign. The combined scheme would serve as a fully automated classifier (the existing classifier requires initial manual identification of lesions by a radiologist), potentially allowing radiologists to reduce their false-positive biopsy rate without reducing their sensitivity for detection of malignancies. Simply concatenating the two types of scheme in a two-stage classifier would be inadequate, because the output of the detection scheme will necessarily include false-positive (FP) computer detections in addition to the malignant and benign lesions to be classified. These FP computer detections correspond to objects which were by design not included in the training sample of the classification scheme, because they are not members of the data population (benign and malignant mass breast lesions) for which the classification scheme was created. It is clear then that the detection scheme's output cannot be used unmodified as the input to the classification scheme.

Our initial efforts toward the goal of developing a true three-class classifier have been more theoretical than practical so far. We have shown that, just as the two-class ideal observer achieves the optimal two-class ROC curve for a given task, the  $N$ -class ideal observer achieves the optimal  $N$ -class ROC hypersurface [18]. (Note that the ideal observer is formally defined as that which minimizes the expected Bayes risk [3], and not in terms of classification performance, making this a non-trivial observation in both cases.) More soberingly, we found recently that an obvious generalization of the well known performance metric, the area under the ROC curve (AUC), is not a useful performance metric in a classification task with three or more classes [19].

At present we are attempting to develop expressions for the coordinates of points on the three-class ideal observer's ROC hypersurface (the conditional probabilities for misclassifying observations [18], [20], [21]) as functions of the set of decision criteria used by the ideal observer. This is considerably more difficult than in the two-class classification task for two reasons. First, the conditional probabilities in question are not simply related to the cumulative distribution functions (cdfs) of the decision variables, but are integrals of those variables over domains determined by three decision boundary lines [3]. Second, the slopes and intercepts of the decision boundary lines are not independent; given the locations of two of the lines, we have found recently that the location of the third will be constrained depending on the other two.

In the present work we attempt to characterize the constraining relationships just mentioned among the three-class ideal observer's decision boundary lines. Although this work is admittedly still removed from image analysis *per se*, we hope it may prove of interest to the CAD community and ultimately of relevance to a wide variety of medical image analysis tasks.

This work was supported by the US Army Medical Research and Materiel Command under Grant W81XWH-04-1-0495 (D. C. Edwards, principal investigator).

\*D. C. Edwards is with the Department of Radiology, the University of Chicago, Chicago, IL, USA (e-mail: d-edwards@uchicago.edu).

C. E. Metz is with the Department of Radiology, the University of Chicago, Chicago, IL, USA.

In the next section we briefly review the structure of the three-class ideal observer and the notation we have been using to characterize it [18]. In Sec. III, we show that for a given location (slope and  $y$ -intercept) of the decision boundary line separating the first and third classes, the location of one of the remaining two lines is constrained in a particular way based on the location of the other.

These results are discussed in Sec. IV. Given the arbitrariness of the labels applied to the three classes (*i. e.*, which classes are considered first, second, or third), one would expect the selection of the fixed line in Sec. III to be similarly arbitrary, and indeed in Appendices A and B we show that corresponding and consistent results are obtained if one takes the location of the decision boundary line separating the second and third, or first and second, classes, respectively, to be given.

## II. THE THREE-CLASS IDEAL OBSERVER

In [18], we showed that an  $N$ -class ideal observer makes decisions by partitioning a likelihood ratio decision variable space, where the boundaries of the partitions are given by hyperplanes:

$$\begin{aligned} \text{decide } d = \pi_i \text{ iff } & \sum_{k=1}^{N-1} (U_{i|k} - U_{j|k})P(\mathbf{t} = \pi_k)\text{LR}_k \\ & \geq (U_{j|N} - U_{i|N})P(\mathbf{t} = \pi_N) \quad \{j < i\} \quad (1) \\ \text{and } & \sum_{k=1}^{N-1} (U_{i|k} - U_{j|k})P(\mathbf{t} = \pi_k)\text{LR}_k \\ & > (U_{j|N} - U_{i|N})P(\mathbf{t} = \pi_N) \quad \{j > i\}. \quad (2) \end{aligned}$$

Here  $U_{i|j}$  is the utility of deciding an observation is from class  $\pi_i$  given that it is actually from class  $\pi_j$ ;  $P(\mathbf{t} = \pi_k)$  is the *a priori* probability that an observation is drawn from class  $\pi_k$ ; and  $\text{LR}_k$  is the  $k$ th likelihood ratio, defined by the ratio  $p(\bar{x}|\pi_k)/p(\bar{x}|\pi_N)$  of the probability density functions of the observational data. The partitioning is determined by the parameters

$$\gamma_{ijk} \equiv (U_{i|k} - U_{j|k})P(\mathbf{t} = \pi_k), \quad (3)$$

with  $i, j$ , and  $k$  varying from 1 to  $N$ , and  $j \neq i$ . Note that these parameters are not independent, however, because

$$\gamma_{ijk} = \gamma_{kjk} - \gamma_{kik}. \quad (4)$$

We can impose the reasonable condition that the utility for correctly classifying an observation from a given class should be greater than any utility for incorrectly classifying an observation from the same class, *i. e.*,  $U_{i|i} > U_{j|i} \quad \{i \neq j\}$ . This gives, for  $j \neq i$ ,

$$\gamma_{iji} > 0, \quad (5)$$

leaving  $N(N-1)$  positive parameters (the rest are derivable from (4)).

Finally, note that the hyperplanes represented by (1) and (2) are unchanged if we multiply all of these equations by a single scalar, such as  $1/(\sum_{i \neq j} \gamma_{iji})$ . This leaves us with  $N^2 - N - 1$  degrees of freedom, as expected.

The behavior of a three-class ideal observer is completely determined by the three decision boundary lines

$$\gamma_{121}\text{LR}_1 - \gamma_{212}\text{LR}_2 = \gamma_{313} - \gamma_{323} \quad (6)$$

$$\gamma_{131}\text{LR}_1 + (\gamma_{232} - \gamma_{212})\text{LR}_2 = \gamma_{313} \quad (7)$$

$$(\gamma_{131} - \gamma_{121})\text{LR}_1 + \gamma_{232}\text{LR}_2 = \gamma_{323}, \quad (8)$$

which we call, respectively, the “1-vs.-2” line, the “1-vs.-3” line, and the “2-vs.-3” line. Note that if any two of these lines intersect, the third line must also share this intersection point. We also emphasize the simple interpretation, from (3), of each of the  $\gamma_{iji}$  parameters appearing in these decision boundary line equations as the difference in utilities between a “correct” and one particular “incorrect” decision (scaled by the *a priori* probability of the true class in question); and of each difference in the  $\gamma_{iji}$  parameters as a difference in utilities between two possible “incorrect” decisions (again scaled by the *a priori* probability of the true class in question; *e. g.*,  $\gamma_{313} - \gamma_{323} = (U_{2|3} - U_{1|3})P(\mathbf{t} = \pi_3)$ ).

From the conditions on the  $\gamma_{iji}$  parameters in (5), we can readily derive conditions on the decision boundaries themselves. If we denote the slope of the “ $i$ -vs.- $j$ ” line by  $m_{ij}$ , its  $y$ -intercept by  $b_{ij}$ , and its  $x$ -intercept by  $\chi_{ij}$ , we have

$$m_{12} = \frac{\gamma_{121}}{\gamma_{212}} > 0 \quad (9)$$

$$\chi_{13} = \frac{\gamma_{313}}{\gamma_{131}} > 0 \quad (10)$$

$$b_{23} = \frac{\gamma_{323}}{\gamma_{232}} > 0. \quad (11)$$

These are the three conditions stated in [22].

## III. RESTRICTIONS DETERMINED BY THE PARAMETERS OF THE “1-VS.-3” LINE

Constraints on the decision boundaries, in addition to those given in (9)–(11), can be obtained by considering the two cases  $\gamma_{232} - \gamma_{212} > 0$  and  $\gamma_{232} - \gamma_{212} < 0$ . In the first case (*i. e.*,  $\gamma_{232} > \gamma_{212}$ , or  $U_{1|2} > U_{3|2}$ ), we have

$$m_{13} = \frac{-\gamma_{131}}{\gamma_{232} - \gamma_{212}} < 0 \quad (12)$$

$$b_{13} = \frac{\gamma_{313}}{\gamma_{232} - \gamma_{212}} > 0. \quad (13)$$

We also have

$$\begin{aligned} m_{23} &= \frac{-(\gamma_{131} - \gamma_{121})}{\gamma_{232}} \\ &= \frac{(\gamma_{232} - \gamma_{212})m_{13} + \gamma_{212}m_{12}}{\gamma_{232}} \\ &= \left(1 - \frac{\gamma_{212}}{\gamma_{232}}\right)m_{13} + \frac{\gamma_{212}}{\gamma_{232}}m_{12}. \quad (14) \end{aligned}$$

This is a weighted sum of the slopes  $m_{12}$  and  $m_{13}$ , where the weights are positive and sum to one. Since we must have  $m_{13} < m_{12}$  from (9) and (12), it must therefore be the case that

$$m_{13} \leq m_{23} \leq m_{12}. \quad (15)$$

Furthermore,

$$\begin{aligned}
b_{23} &= \frac{\gamma_{323}}{\gamma_{232}} \\
&= \frac{\gamma_{313} - (\gamma_{313} - \gamma_{323})}{\gamma_{232}} \\
&= \frac{(\gamma_{232} - \gamma_{212})b_{13} + \gamma_{212}b_{12}}{\gamma_{232}} \\
&= \left(1 - \frac{\gamma_{212}}{\gamma_{232}}\right)b_{13} + \frac{\gamma_{212}}{\gamma_{232}}b_{12}. \quad (16)
\end{aligned}$$

This is a weighted sum of the  $y$ -intercepts  $b_{12}$  and  $b_{13}$ , where the weights are positive and sum to one; thus, in addition to (15), we have the condition

$$\min(b_{12}, b_{13}) \leq b_{23} \leq \max(b_{12}, b_{13}). \quad (17)$$

If  $b_{12} < 0$ , then (17) immediately reduces to  $b_{12} \leq b_{23} \leq b_{13}$  (by (13), we are considering a special case in which  $b_{13} > 0$ ). This is illustrated in Fig. 1 for the slightly different situations  $\chi_{12} < \chi_{13}$  and  $\chi_{12} \geq \chi_{13}$ . If, on the other hand,  $b_{12} \geq 0$ , then (15) and (17) together imply two possible situations, depending on whether  $b_{12} < b_{13}$  or  $b_{12} \geq b_{13}$ . These possibilities are illustrated in Fig. 2.

We now consider the case  $\gamma_{232} - \gamma_{212} < 0$  (*i. e.*,  $\gamma_{232} < \gamma_{212}$ , or  $U_{1|2} < U_{3|2}$ ), which yields

$$m_{13} = \frac{-\gamma_{131}}{\gamma_{232} - \gamma_{212}} > 0 \quad (18)$$

$$b_{13} = \frac{\gamma_{313}}{\gamma_{232} - \gamma_{212}} < 0. \quad (19)$$

We now have

$$\begin{aligned}
m_{12} &= \frac{\gamma_{121}}{\gamma_{212}} \\
&= \frac{\gamma_{131} - (\gamma_{131} - \gamma_{121})}{\gamma_{212}} \\
&= \frac{-(\gamma_{232} - \gamma_{212})m_{13} + \gamma_{232}m_{23}}{\gamma_{212}} \\
&= \left(1 - \frac{\gamma_{232}}{\gamma_{212}}\right)m_{13} + \frac{\gamma_{232}}{\gamma_{212}}m_{23}. \quad (20)
\end{aligned}$$

This is again a weighted sum in which the weights are positive and sum to one, giving

$$\min(m_{13}, m_{23}) \leq m_{12} \leq \max(m_{13}, m_{23}). \quad (21)$$

Furthermore,

$$\begin{aligned}
b_{12} &= \frac{\gamma_{313} - \gamma_{323}}{-\gamma_{212}} \\
&= \frac{-\gamma_{313} + \gamma_{323}}{\gamma_{212}} \\
&= \frac{-(\gamma_{232} - \gamma_{212})b_{13} + \gamma_{232}b_{23}}{\gamma_{212}} \\
&= \left(1 - \frac{\gamma_{232}}{\gamma_{212}}\right)b_{13} + \frac{\gamma_{232}}{\gamma_{212}}b_{23}. \quad (22)
\end{aligned}$$

This is a weighted sum of the  $y$ -intercepts  $b_{13}$  and  $b_{23}$ , where the weights are positive and sum to one; thus, in addition to (21), we have the condition

$$b_{13} \leq b_{12} \leq b_{23}, \quad (23)$$

since  $b_{13} < b_{23}$  by (11) and (19).

If  $m_{23} < 0$ , then (21) immediately reduces to  $m_{23} \leq m_{12} \leq m_{13}$  (by (18), we are considering a special case in which  $m_{13} > 0$ ). This is illustrated in Fig. 3 for the slightly different situations  $\chi_{13} < \chi_{23}$  and  $\chi_{13} \geq \chi_{23}$ . If, on the other hand,  $m_{23} \geq 0$ , then (21) and (23) together imply two possible situations, depending on whether  $m_{23} < m_{13}$  or  $m_{23} \geq m_{13}$ . These possibilities are illustrated in Fig. 4.

One may of course ask what happens when  $\gamma_{232} - \gamma_{212} = 0$  (*i. e.*,  $\gamma_{232} = \gamma_{212}$ , or  $U_{1|2} = U_{3|2}$ ). In this case, both  $m_{13}$  and  $b_{13}$  are infinite. Furthermore,

$$\begin{aligned}
m_{23} &= \frac{-(\gamma_{131} - \gamma_{121})}{\gamma_{232}} \\
&= \frac{-\gamma_{131}}{\gamma_{232}} + \frac{\gamma_{121}}{\gamma_{212}} \\
&= \frac{-\gamma_{131}}{\gamma_{232}} + m_{12} \\
&\leq m_{12}, \quad (24)
\end{aligned}$$

and

$$\begin{aligned}
b_{12} &= \frac{\gamma_{323} - \gamma_{313}}{\gamma_{212}} \\
&= \frac{\gamma_{323}}{\gamma_{232}} + \frac{-\gamma_{313}}{\gamma_{212}} \\
&= b_{23} + \frac{-\gamma_{313}}{\gamma_{212}} \\
&\leq b_{23}. \quad (25)
\end{aligned}$$

Together, (24) and (25) can be considered *either* a special case of the inequalities (15) and (17), if we take  $m_{13} = -\infty$  and  $b_{13} = +\infty$ ; *or* of the inequalities (21) and (23), if we take  $m_{13} = +\infty$  and  $b_{13} = -\infty$ . This situation, for the slightly different cases  $b_{12} < 0$  and  $b_{12} \geq 0$ , is illustrated in Fig. 5.

In this section, the possible values of the quantity  $\gamma_{232} - \gamma_{212}$  were considered in order to determine properties of the ideal observer decision boundary lines. It may be argued that the choice of a parameter from the “1-vs.-3” line, *i. e.*, one of the three available lines, must be an arbitrary one. In fact, we may consider taking another parameter (or combination of parameters) from (6)–(8), and using it to determine conditions on the properties of the decision boundary lines as above. Given that all possible values of the quantity  $\gamma_{232} - \gamma_{212}$  were considered, it is expected that no new conditions should be determinable (let alone conditions inconsistent with those already determined). In fact, this can readily be shown to be the case; however, due to the repetitive nature of the derivations involved, these are relegated to Appendices A and B.

#### IV. DISCUSSION AND CONCLUSIONS

The repetitive nature of the algebraic manipulations given in the preceding section and the appendices should not be allowed to distract from the fundamental point being made: given the locations of two of the decision boundary lines, the location of the third is not completely arbitrary. That is, aside from the obvious (given (6)–(8)) constraint that the lines must share a common intersection point, it can also be shown that

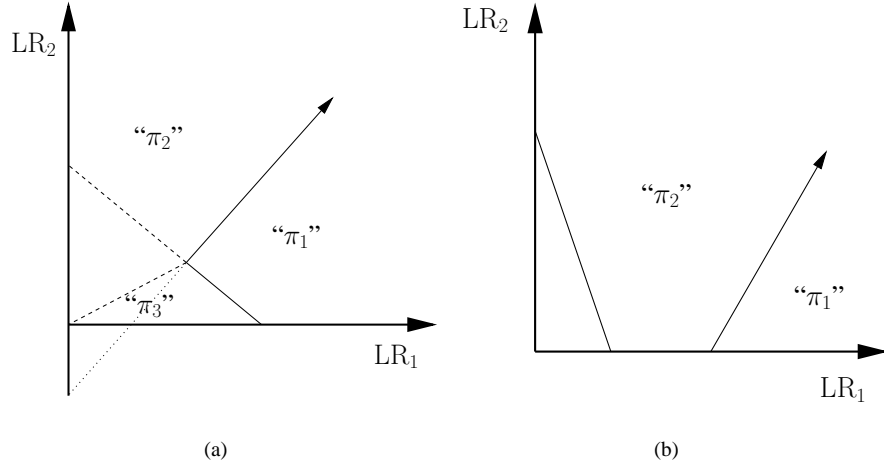


Fig. 1. Example ideal observer decision rules for the case  $\gamma_{232} - \gamma_{212} > 0$  (implying  $m_{13} < 0$  and  $b_{13} > 0$ ) and  $b_{12} < 0$ . In (a),  $\chi_{12} < \chi_{13}$ , and the “2-vs.-3” line can lie anywhere between the two dashed lines shown (the region between the lower dashed and dotted lines is excluded because  $b_{23} > 0$ ); observations in the unlabeled region above this line will be decided “π<sub>2</sub>”, and those below this line will be decided “π<sub>3</sub>”. In (b),  $\chi_{12} \geq \chi_{13}$ , and the “2-vs.-3” line can lie anywhere in the unlabeled region (provided it shares the intersection point of the “1-vs.-2” and “1-vs.-3” lines shown); observations above this line will be decided “π<sub>2</sub>”, and those below this line will be decided “π<sub>3</sub>”.

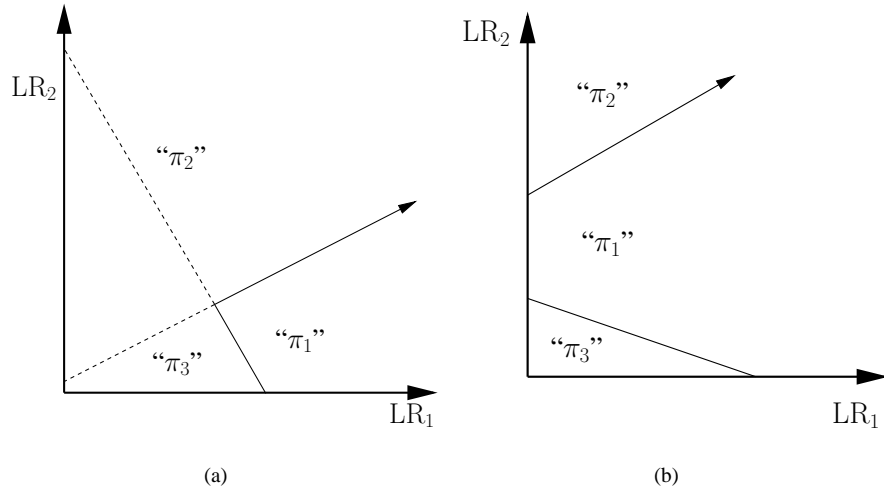


Fig. 2. Example ideal observer decision rules for the case  $\gamma_{232} - \gamma_{212} > 0$  (implying  $m_{13} < 0$  and  $b_{13} > 0$ ) and  $b_{12} \geq 0$ . In (a),  $b_{12} < b_{13}$ , and the “2-vs.-3” line can lie anywhere in the unlabeled region; observations above this line will be decided “π<sub>2</sub>”, and those below this line will be decided “π<sub>3</sub>”. In (b),  $b_{12} \geq b_{13}$ , and the “2-vs.-3” line can lie anywhere between the “1-vs.-2” and “1-vs.-3” lines (provided it shares their intersection point); note that observations in this region will be decided “π<sub>1</sub>” regardless of the position of this line.

the slope of the third line is constrained by the slopes of the first two.

The significance of this result may be difficult to appreciate at first glance. It is perhaps best illustrated by comparison with the two-class classifier, for which the ROC operating point coordinates (*e. g.*, the true-positive fraction (TPF) and false-positive fraction (FPF)) are determined by a single decision criterion  $\gamma$ , which is free to vary without restriction throughout its domain of definition. For the two-class ideal observer, in particular, an observation is decided “positive” (assigned to the class  $\pi_1$ ) if  $LR_1 > \gamma$ , where  $\gamma$  can take on any nonnegative value. Furthermore, the FPF and TPF are related in a very simple way to the cdfs of  $LR_1$ , and are thus monotonic in the decision criterion  $\gamma$ . For the three-class ideal observer, this

straightforward relationship is lost; indeed, Figs. 2(b), 4(b), 7(b), 9(b), 12(b), and 14(b) show that for certain values of four of the five decision criteria  $\gamma_{ijj}$ , the misclassification probabilities (*i. e.*, the ROC operating point coordinates) can be independent of the fifth decision criterion.

More succinctly, the relationship between the decision criteria and the misclassification probabilities is *not* one-to-one, as it is for the two-class ideal observer. A correct formulation of the misclassification probabilities as functions of the decision criteria — necessary for an explicit calculation of the ideal observer’s ROC hypersurface given the decision variable probability density functions — will require careful consideration of this issue. Although we have shown previously that the hypervolume under the ROC hypersurface is not a useful

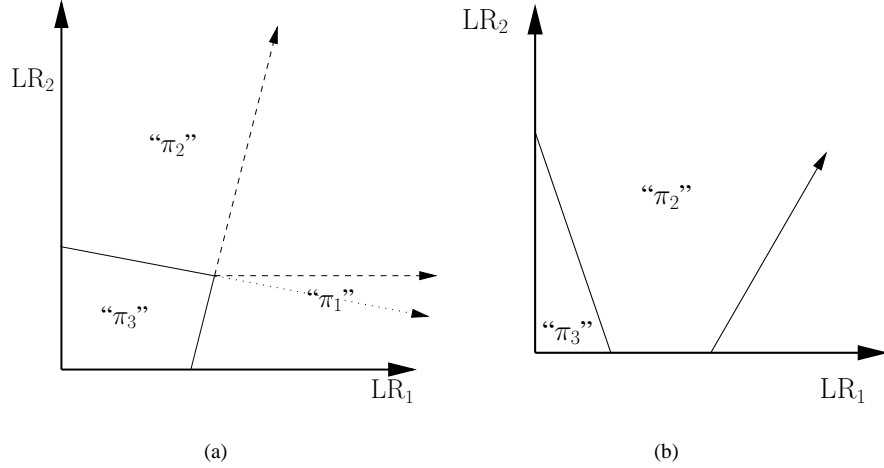


Fig. 3. Example ideal observer decision rules for the case  $\gamma_{232} - \gamma_{212} < 0$  (implying  $m_{13} > 0$  and  $b_{13} < 0$ ) and  $m_{23} < 0$ . In (a),  $\chi_{13} < \chi_{23}$ , and the “1-vs.-2” line can lie anywhere between the two dashed lines shown (the region between the lower dashed and dotted lines is excluded because  $m_{12} > 0$ ); observations in the unlabeled region above this line will be decided “ $\pi_2$ ”, and those below this line will be decided “ $\pi_1$ ”. In (b),  $\chi_{13} \geq \chi_{23}$ , and the “1-vs.-2” line can lie anywhere in the unlabeled region (provided it shares the intersection point of the “1-vs.-3” and “2-vs.-3” lines shown); observations above this line will be decided “ $\pi_2$ ”, and those below this line will be decided “ $\pi_1$ ”.

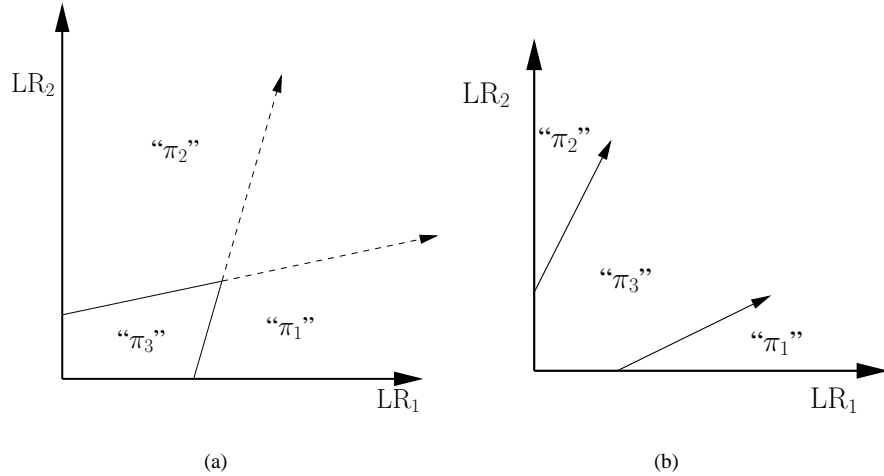


Fig. 4. Example ideal observer decision rules for the case  $\gamma_{232} - \gamma_{212} < 0$  (implying  $m_{13} > 0$  and  $b_{13} < 0$ ) and  $m_{23} \geq 0$ . In (a),  $m_{23} < m_{13}$ , and the “1-vs.-2” line can lie anywhere in the unlabeled region; observations above this line will be decided “ $\pi_2$ ”, and those below this line will be decided “ $\pi_1$ ”. In (b),  $m_{23} \geq m_{13}$ , and the “1-vs.-2” line can lie anywhere between the “1-vs.-3” and “2-vs.-3” lines (provided it shares their intersection point); note that observations in this region will be decided “ $\pi_3$ ” regardless of the position of this line.

performance metric in general [19], it is still the case that the ROC hypersurface in terms of the set of misclassification probabilities (six in the three-class classification task) is a complete description of observer performance. We expect that a useful performance metric, assuming one exists, will be derived in some fashion from the ROC hypersurface. It is thus important to develop a complete understanding of the rather complicated relationships among the quantities involved, and we hope that the present work will prove of some use toward this goal.

#### APPENDIX A RESTRICTIONS DETERMINED BY THE PARAMETERS OF THE “2-VS.-3” LINE

Consider the quantity  $\gamma_{131} - \gamma_{121}$  from (8). In particular, when  $\gamma_{131} - \gamma_{121} > 0$  (i. e.,  $\gamma_{131} > \gamma_{121}$ , or  $U_{2|1} > U_{3|1}$ ), we have

$$\frac{1}{m_{23}} = \frac{-\gamma_{232}}{\gamma_{131} - \gamma_{121}} < 0 \quad (26)$$

$$\chi_{23} = \frac{\gamma_{323}}{\gamma_{131} - \gamma_{121}} > 0. \quad (27)$$

Through reasoning similar to that of Sec. III, we also have

$$\frac{1}{m_{23}} \leq \frac{1}{m_{13}} \leq \frac{1}{m_{12}} \quad (28)$$

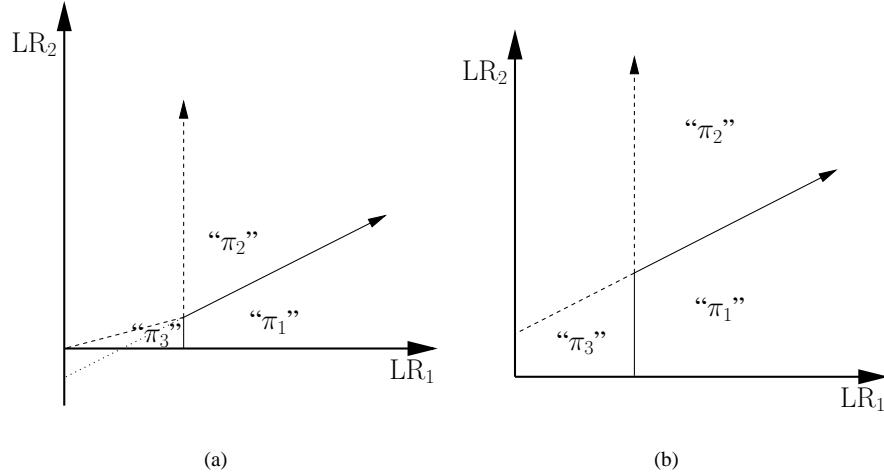


Fig. 5. Example ideal observer decision rules for the case  $\gamma_{232} - \gamma_{212} = 0$  (implying  $m_{13} = \mp\infty$  and  $b_{13} = \pm\infty$ ). In (a),  $b_{12} < 0$ , and the “2-vs.-3” line can lie anywhere between the two dashed lines shown (the region between the lower dashed and dotted lines is excluded because  $b_{23} > 0$ ); observations in the unlabeled region above this line will be decided “ $\pi_2$ ”, and those below this line will be decided “ $\pi_3$ ”. In (b),  $b_{12} \geq 0$ , and the “2-vs.-3” line can lie anywhere in the unlabeled region; observations above this line will be decided “ $\pi_2$ ”, and those below this line will be decided “ $\pi_3$ ”.

and

$$\min(\chi_{12}, \chi_{23}) \leq \chi_{13} \leq \max(\chi_{12}, \chi_{23}). \quad (29)$$

If  $\chi_{12} < 0$ , then (29) immediately reduces to  $\chi_{12} \leq \chi_{13} \leq \chi_{23}$  (by (27), we are considering a special case in which  $\chi_{23} > 0$ ). This is illustrated in Fig. 6 for the slightly different situations  $b_{12} < b_{23}$  and  $b_{12} \geq b_{23}$ . If, on the other hand,  $\chi_{12} \geq 0$ , then (28) and (29) together imply two possible situations, depending on whether  $\chi_{12} < \chi_{23}$  or  $\chi_{12} \geq \chi_{23}$ . These possibilities are illustrated in Fig. 7.

If  $\gamma_{131} - \gamma_{121} < 0$  (i. e.,  $\gamma_{131} < \gamma_{121}$ , or  $U_{2|1} < U_{3|1}$ ), we have

$$\frac{1}{m_{23}} = \frac{-\gamma_{232}}{\gamma_{131} - \gamma_{121}} > 0 \quad (30)$$

$$\chi_{23} = \frac{\gamma_{323}}{\gamma_{131} - \gamma_{121}} < 0. \quad (31)$$

One can also show

$$\min\left(\frac{1}{m_{13}}, \frac{1}{m_{23}}\right) \leq \frac{1}{m_{12}} \leq \max\left(\frac{1}{m_{13}}, \frac{1}{m_{23}}\right) \quad (32)$$

and

$$\chi_{23} \leq \chi_{12} \leq \chi_{13}. \quad (33)$$

If  $1/m_{13} < 0$ , then (32) immediately reduces to  $1/m_{13} \leq 1/m_{12} \leq 1/m_{23}$  (by (30), we are considering a special case in which  $1/m_{23} > 0$ ). This is illustrated in Fig. 8 for the slightly different situations  $b_{23} < b_{13}$  and  $b_{23} \geq b_{13}$ . If, on the other hand,  $1/m_{13} \geq 0$ , then (32) and (33) together imply two possible situations, depending on whether  $1/m_{13} < 1/m_{23}$  or  $1/m_{13} \geq 1/m_{23}$ . These possibilities are illustrated in Fig. 9.

Finally, we consider the case  $\gamma_{131} - \gamma_{121} = 0$  ( $\gamma_{131} = \gamma_{121}$ , or  $U_{2|1} = U_{3|1}$ ), in which both  $1/m_{23}$  and  $\chi_{23}$  are infinite. We now have

$$\frac{1}{m_{13}} \leq \frac{1}{m_{12}} \quad (34)$$

and

$$\chi_{12} \leq \chi_{13}. \quad (35)$$

Together, (34) and (35) can be considered *either* a special case of the inequalities (28) and (29), if we take  $1/m_{23} = -\infty$  and  $\chi_{23} = +\infty$ ; *or* of the inequalities (32) and (33), if we take  $1/m_{23} = +\infty$  and  $\chi_{23} = -\infty$ . This situation, for the slightly different cases  $\chi_{12} < 0$  and  $\chi_{12} \geq 0$ , is illustrated in Fig. 10.

Notice that every figure in this appendix has one or more corresponding figures in Sec. III (depending on the possible values of the undetermined decision boundary parameter being illustrated in that figure). Specifically,

Fig. 6(a)  $\Rightarrow$  Figs. 2(a), 3(a), 5(b)

Fig. 6(b)  $\Rightarrow$  Fig. 2(b)

Fig. 7(a)  $\Rightarrow$  Figs. 1(a), 3(a), 5(a)

Fig. 7(b)  $\Rightarrow$  Figs. 1(b), 3(b), 5(a)

Fig. 8(a)  $\Rightarrow$  Figs. 1(a), 2(a)

Fig. 8(b)  $\Rightarrow$  Fig. 2(b)

Fig. 9(a)  $\Rightarrow$  Figs. 4(a), 5(a), 5(b)

Fig. 9(b)  $\Rightarrow$  Fig. 4(b)

Fig. 10(a)  $\Rightarrow$  Figs. 2(a), 4(a), 5(b), 2(b)

Fig. 10(b)  $\Rightarrow$  Figs. 1(a), 4(a), 5(a)

That is, none of the conditions derived in this section are inconsistent with those derived Sec. III. More importantly, note the symmetry between the corresponding equations and figures in Sec. III and this appendix, if one “swaps” the labels of classes  $\pi_1$  and  $\pi_2$ , and additionally replaces  $m_{ij}$  with  $1/m_{i'j'}$ ,  $\chi_{ij}$  with  $b_{i'j'}$ , and  $b_{ij}$  with  $\chi_{i'j'}$  ( $i' = 1$  if  $i = 2$ , 2 if  $i = 1$ , and 3 if  $i = 3$ ; similarly for  $j$ ). Intuitively, if one “flips” the figures in one section about the  $y = x$  line, one obtains the figures in the other section.

## APPENDIX B

### RESTRICTIONS DETERMINED BY THE PARAMETERS OF THE “1-vs.-2” LINE

In this appendix, we consider the possible values of the quantity  $\gamma_{313} - \gamma_{323}$ . As in the preceding appendix, we expect to obtain no conditions inconsistent with those already derived.

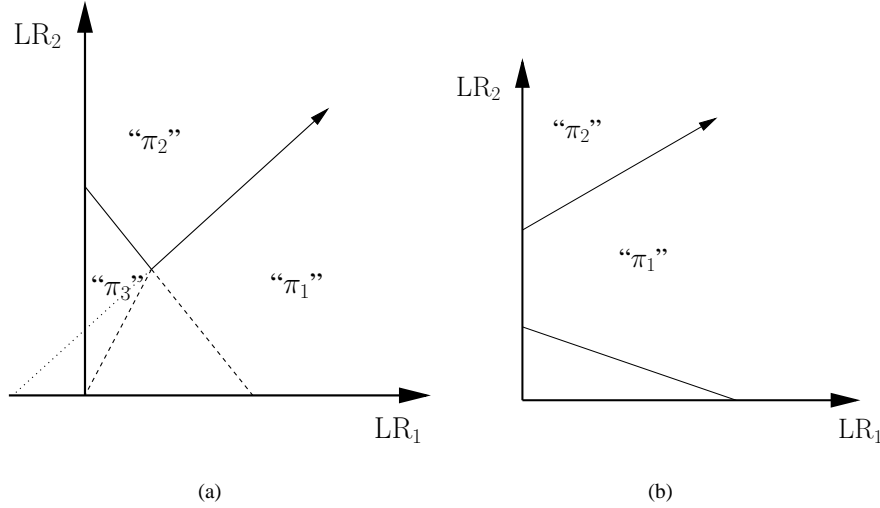


Fig. 6. Example ideal observer decision rules for the case  $\gamma_{131} - \gamma_{121} > 0$  (implying  $1/m_{23} < 0$  and  $\chi_{23} > 0$ ) and  $\chi_{12} < 0$ . In (a),  $b_{12} < b_{23}$ , and the “1-vs.-3” line can lie anywhere between the two dashed lines shown (the region between the left dashed and dotted lines is excluded because  $\chi_{13} > 0$ ); observations in the unlabeled region to the right of this line will be decided “ $\pi_1$ ”, and those to the left of this line will be decided “ $\pi_3$ ”. In (b),  $b_{12} \geq b_{23}$ , and the “1-vs.-3” line can lie anywhere in the unlabeled region (provided it shares the intersection point of the “1-vs.-2” and “2-vs.-3” lines shown); observations to the right of this line will be decided “ $\pi_1$ ”, and those to the left of this line will be decided “ $\pi_3$ ”.

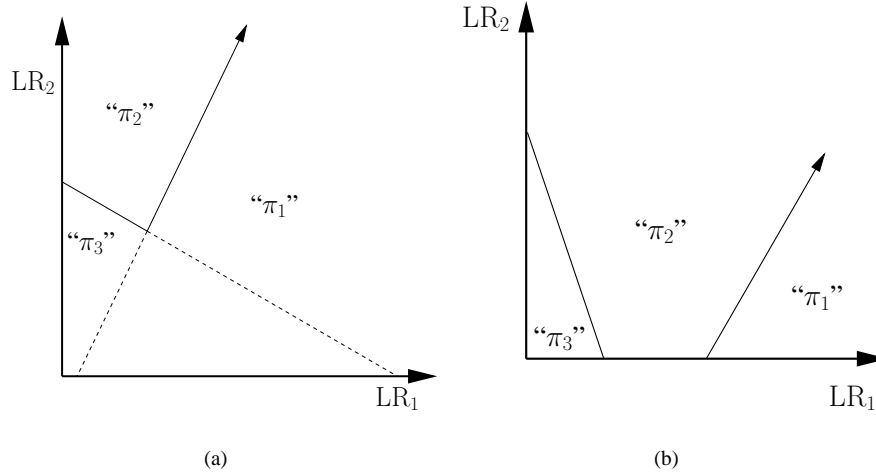


Fig. 7. Example ideal observer decision rules for the case  $\gamma_{131} - \gamma_{121} > 0$  (implying  $1/m_{23} < 0$  and  $\chi_{23} > 0$ ) and  $\chi_{12} \geq 0$ . In (a),  $\chi_{12} < \chi_{23}$ , and the “1-vs.-3” line can lie anywhere in the unlabeled region; observations to the left of this line will be decided “ $\pi_3$ ”, and those to the right of this line will be decided “ $\pi_1$ ”. In (b),  $\chi_{12} \geq \chi_{23}$ , and the “1-vs.-3” line can lie anywhere between the “1-vs.-2” and “2-vs.-3” lines (provided it shares their intersection point); note that observations in this region will be decided “ $\pi_2$ ” regardless of the position of this line.

When  $\gamma_{313} - \gamma_{323} > 0$  (i. e.,  $\gamma_{313} > \gamma_{323}$ , or  $U_{2|3} > U_{1|3}$ ), we have

$$\frac{1}{b_{12}} = \frac{-\gamma_{212}}{\gamma_{313} - \gamma_{323}} < 0 \quad (36)$$

$$\frac{1}{\chi_{12}} = \frac{\gamma_{121}}{\gamma_{313} - \gamma_{323}} > 0. \quad (37)$$

Through reasoning similar to that of Sec. III, we also have

$$\frac{1}{b_{12}} \leq \frac{1}{b_{13}} \leq \frac{1}{b_{23}} \quad (38)$$

and

$$\min\left(\frac{1}{\chi_{23}}, \frac{1}{\chi_{12}}\right) \leq \frac{1}{\chi_{13}} \leq \max\left(\frac{1}{\chi_{23}}, \frac{1}{\chi_{12}}\right). \quad (39)$$

If  $1/\chi_{23} \leq 0$ , then (39) immediately reduces to  $1/\chi_{23} \leq 1/\chi_{13} \leq 1/\chi_{12}$  (by (37), we are considering a special case in which  $1/\chi_{12} > 0$ ). This is illustrated in Fig. 11 for the slightly different situations  $m_{23} < m_{12}$  and  $m_{23} \geq m_{12}$ . If, on the other hand,  $1/\chi_{23} > 0$ , then (38) and (39) together imply two possible situations, depending on whether  $1/\chi_{23} < 1/\chi_{12}$  or  $1/\chi_{23} \geq 1/\chi_{12}$ . These possibilities are illustrated in Fig. 12.

If  $\gamma_{313} - \gamma_{323} < 0$  (i. e.,  $\gamma_{313} < \gamma_{323}$ , or  $U_{2|3} < U_{1|3}$ ), we have

$$\frac{1}{b_{12}} = \frac{-\gamma_{212}}{\gamma_{313} - \gamma_{323}} > 0 \quad (40)$$

$$\frac{1}{\chi_{12}} = \frac{\gamma_{121}}{\gamma_{313} - \gamma_{323}} < 0. \quad (41)$$

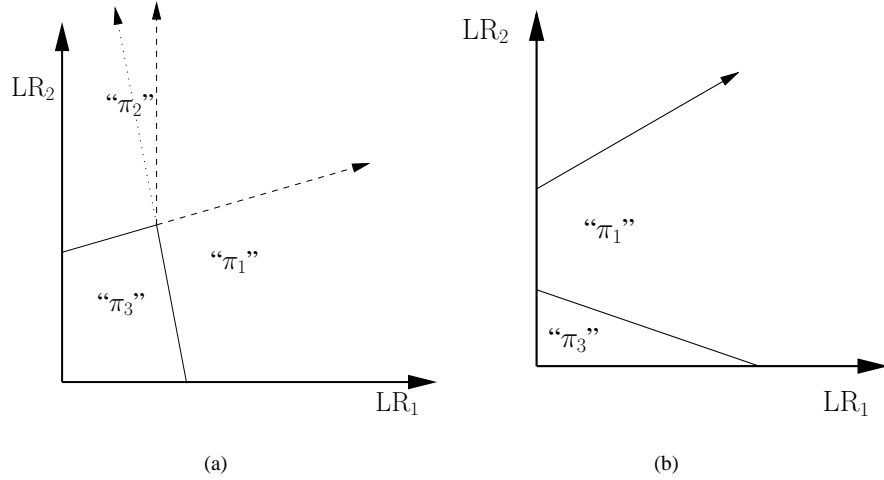


Fig. 8. Example ideal observer decision rules for the case  $\gamma_{131} - \gamma_{121} < 0$  (implying  $1/m_{23} > 0$  and  $\chi_{23} < 0$ ) and  $1/m_{13} < 0$ . In (a),  $b_{23} < b_{13}$ , and the “1-vs.-2” line can lie anywhere between the two dashed lines shown (the region between the vertical dashed and dotted lines is excluded because  $m_{12} > 0$ , and therefore  $1/m_{12} \geq 0$ ); observations in the unlabeled region above this line will be decided “ $\pi_2$ ”, and those below this line will be decided “ $\pi_1$ ”. In (b),  $b_{23} \geq b_{13}$ , and the “1-vs.-2” line can lie anywhere in the unlabeled region (provided it shares the intersection point of the “1-vs.-3” and “2-vs.-3” lines shown); observations above this line will be decided “ $\pi_2$ ”, and those below this line will be decided “ $\pi_1$ ”.

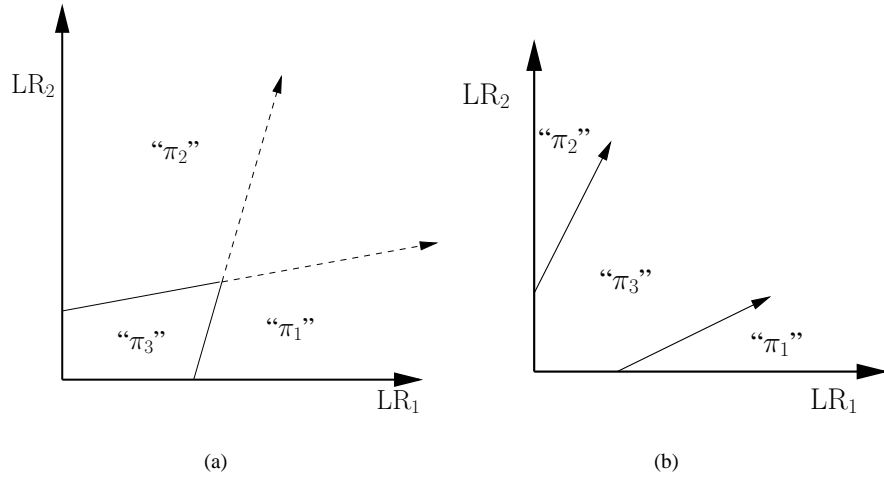


Fig. 9. Example ideal observer decision rules for the case  $\gamma_{131} - \gamma_{121} < 0$  (implying  $1/m_{23} > 0$  and  $\chi_{23} < 0$ ) and  $1/m_{13} \geq 0$ . In (a),  $1/m_{13} < 1/m_{23}$ , and the “1-vs.-2” line can lie anywhere in the unlabeled region; observations above this line will be decided “ $\pi_2$ ”, and those below this line will be decided “ $\pi_1$ ”. In (b),  $1/m_{13} \geq 1/m_{23}$ , and the “1-vs.-2” line can lie anywhere between the “1-vs.-3” and “2-vs.-3” lines (provided it shares their intersection point); note that observations in this region will be decided “ $\pi_3$ ” regardless of the position of this line.

One can also show

$$\min\left(\frac{1}{b_{13}}, \frac{1}{b_{12}}\right) \leq \frac{1}{b_{23}} \leq \max\left(\frac{1}{b_{13}}, \frac{1}{b_{12}}\right) \quad (42)$$

and

$$\frac{1}{\chi_{12}} \leq \frac{1}{\chi_{23}} \leq \frac{1}{\chi_{13}}. \quad (43)$$

If  $1/b_{13} \leq 0$ , then (42) immediately reduces to  $1/b_{13} \leq 1/b_{23} \leq 1/b_{12}$  (by (40), we are considering a special case in which  $1/b_{12} > 0$ ). This is illustrated in Fig. 13 for the slightly different situations  $m_{12} < m_{13}$  and  $m_{12} \geq m_{13}$ . If, on the other hand,  $1/b_{13} > 0$ , then (42) and (43) together imply two possible situations, depending on whether  $1/b_{13} < 1/b_{12}$  or  $1/b_{13} \geq 1/b_{12}$ . These possibilities are illustrated in Fig. 14.

Finally, we consider the case  $\gamma_{323} - \gamma_{313} = 0$  (i. e.,  $\gamma_{313} = \gamma_{323}$ , or  $U_{2|3} = U_{1|3}$ ), in which both  $1/b_{12}$  and  $1/\chi_{12}$  are infinite. We now have

$$\frac{1}{b_{13}} \leq \frac{1}{b_{23}} \quad (44)$$

$$\frac{1}{\chi_{23}} \leq \frac{1}{\chi_{13}}. \quad (45)$$

Together, (44) and (45) can be considered *either* a special case of the inequalities (38) and (39), if we take  $1/b_{12} = -\infty$  and  $1/\chi_{12} = +\infty$ ; *or of* the inequalities (42) and (43), if we take  $1/b_{12} = +\infty$  and  $1/\chi_{12} = -\infty$ . This situation, for the slightly different cases  $1/b_{13} \leq 0$  and  $1/b_{13} > 0$ , is illustrated in Fig. 15.

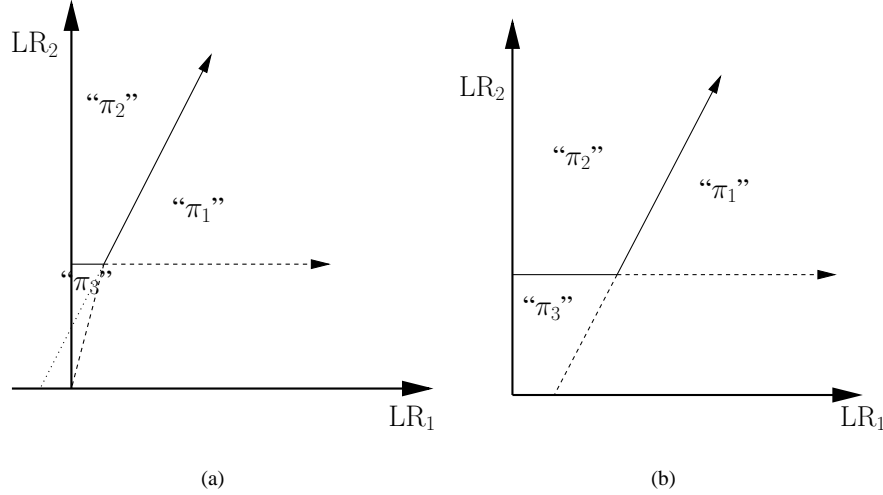


Fig. 10. Example ideal observer decision rules for the case  $\gamma_{131} - \gamma_{121} = 0$  (implying  $1/m_{23} = \mp\infty$  and  $\chi_{23} = \pm\infty$ ). In (a),  $\chi_{12} < 0$ , and the “1-vs.-3” line can lie anywhere between the two dashed lines shown (the region between the leftmost dashed and dotted lines is excluded because  $\chi_{13} > 0$ ); observations in the unlabeled region to the right of this line will be decided “ $\pi_1$ ”, and those to the left of this line will be decided “ $\pi_3$ ”. In (b),  $\chi_{12} \geq 0$ , and the “1-vs.-3” line can lie anywhere in the unlabeled region; observations to the right of this line will be decided “ $\pi_1$ ”, and those to the left of this line will be decided “ $\pi_3$ ”.

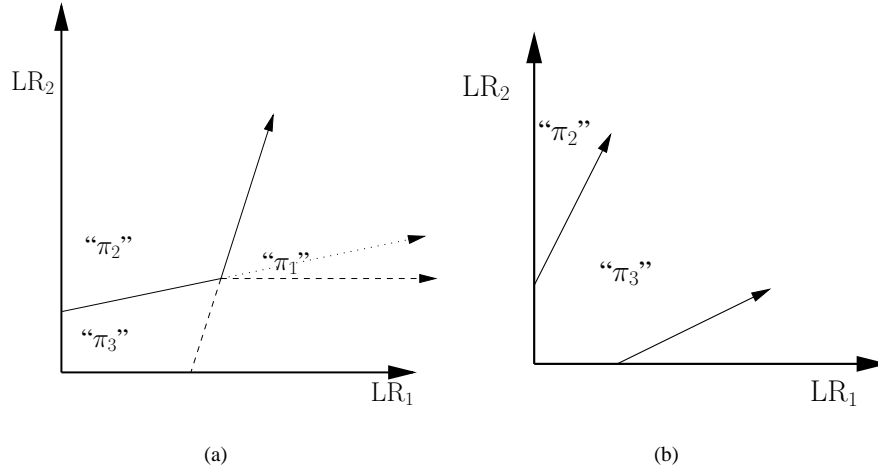


Fig. 11. Example ideal observer decision rules for the case  $\gamma_{313} - \gamma_{323} > 0$  (implying  $1/b_{12} < 0$  and  $1/\chi_{12} > 0$ ) and  $1/\chi_{23} \leq 0$ . In (a),  $m_{23} < m_{12}$ , and the “1-vs.-3” line can lie anywhere between the two dashed lines shown (the region between the horizontal dashed and dotted lines is excluded because  $\chi_{13} > 0$ , and therefore  $1/\chi_{13} \geq 0$ ); observations in the unlabeled region to the left of this line will be decided “ $\pi_3$ ”, and those to the right of line will be decided “ $\pi_1$ ”. In (b),  $m_{23} \geq m_{12}$ , and the “1-vs.-3” line can lie anywhere in the unlabeled region (provided it shares the intersection point of the “1-vs.-2” and “2-vs.-3” lines shown); observations to the left of this line will be decided “ $\pi_3$ ”, and those to the right of this line will be decided “ $\pi_1$ ”.

Notice that every figure in this appendix has one or more corresponding figures in Sec. III (depending on the possible values of the undetermined decision boundary parameter being illustrated in that figure). Specifically,

- Fig. 11(a)  $\Rightarrow$  Figs. 1(a), 4(a), 5(a)
- Fig. 11(b)  $\Rightarrow$  Fig. 4(b)
- Fig. 12(a)  $\Rightarrow$  Figs. 1(a), 3(a), 5(a)
- Fig. 12(b)  $\Rightarrow$  Figs. 1(b), 3(b), 5(a)
- Fig. 13(a)  $\Rightarrow$  Figs. 3(a), 4(a), 5(b)
- Fig. 13(b)  $\Rightarrow$  Fig. 4(b)
- Fig. 14(a)  $\Rightarrow$  Fig. 2(a)
- Fig. 14(b)  $\Rightarrow$  Fig. 2(b)
- Fig. 15(a)  $\Rightarrow$  Figs. 3(a), 4(a), 5(b)
- Fig. 15(b)  $\Rightarrow$  Figs. 2(a), 3(a), 4(b)

That is, none of the conditions derived in this appendix are inconsistent with those derived in Sec. III or Appendix A. More importantly, note the symmetry between the correspond-

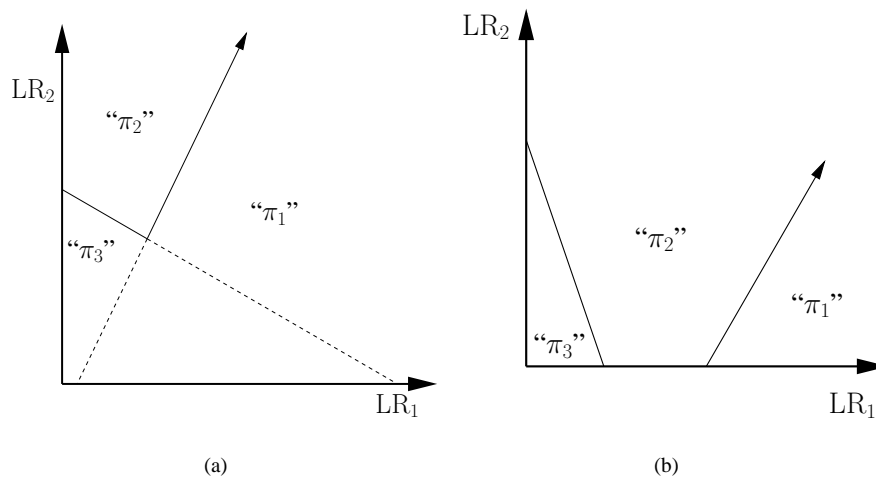


Fig. 12. Example ideal observer decision rules for the case  $\gamma_{313} - \gamma_{323} > 0$  (implying  $1/b_{12} < 0$  and  $1/\chi_{12} > 0$ ) and  $1/\chi_{23} > 0$ . In (a),  $1/\chi_{23} < 1/\chi_{12}$ , and the “1-vs.-3” line can lie anywhere in the unlabeled region; observations to the left of this line will be decided “ $\pi_3$ ”, and those to the right of this line will be decided “ $\pi_1$ ”. In (b),  $1/\chi_{23} \geq 1/\chi_{12}$ , and the “1-vs.-3” line can lie anywhere between the “1-vs.-2” and “2-vs.-3” lines (provided it shares their intersection point); note that observations in this region will be decided “ $\pi_2$ ” regardless of the position of this line.

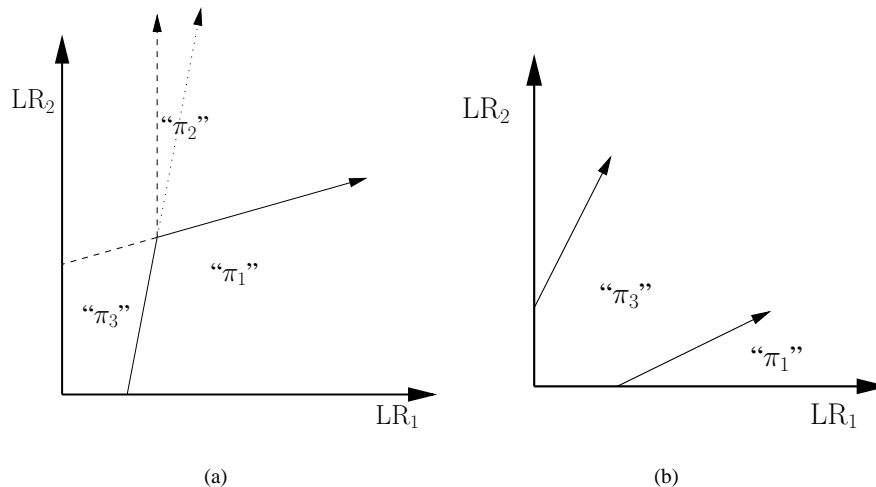


Fig. 13. Example ideal observer decision rules for the case  $\gamma_{313} - \gamma_{323} < 0$  (implying  $1/b_{12} > 0$  and  $1/\chi_{12} < 0$ ) and  $1/b_{13} \leq 0$ . In (a),  $m_{12} < m_{13}$ , and the “2-vs.-3” line can lie anywhere between the two dashed lines shown (the region between the vertical dashed and dotted lines is excluded because  $b_{23} > 0$ , and therefore  $1/b_{23} \geq 0$ ); observations in the unlabeled region above this line will be decided “ $\pi_2$ ”, and those below this line will be decided “ $\pi_3$ ”. In (b),  $m_{12} \geq m_{13}$ , and the “2-vs.-3” line can lie anywhere in the unlabeled region (provided it shares the intersection point of the “1-vs.-2” and “1-vs.-3” lines shown); observations above this line will be decided “ $\pi_2$ ”, and those below this line will be decided “ $\pi_3$ ”.

ing equations and figures in Secs. III and this appendix, if one “swaps” the labels of classes  $\pi_2$  and  $\pi_3$ , and additionally replaces  $m_{ij}$  with  $1/\chi_{i'j'}$ ,  $\chi_{ij}$  with  $1/m_{i'j'}$ , and  $b_{ij}$  with  $1/b_{i'j'}$  ( $i' = 1$  if  $i = 1$ , 2 if  $i = 3$ , and 3 if  $i = 2$ ; similarly for  $j$ ).

#### ACKNOWLEDGMENTS

The authors thank the associate editor and anonymous reviewers for their suggestions to substantially improve the content and structure of this manuscript.

#### REFERENCES

- [1] J. P. Egan, *Signal Detection Theory and ROC Analysis*. New York: Academic Press, 1975.
- [2] C. E. Metz, “Basic principles of ROC analysis,” *Seminars in Nuclear Medicine*, vol. VIII, no. 4, pp. 283–298, 1978.
- [3] H. L. Van Trees, *Detection, Estimation and Modulation Theory: Part I*. New York: John Wiley & Sons, 1968.
- [4] B. K. Scurfield, “Multiple-event forced-choice tasks in the theory of signal detectability,” *J. Math Psychol.*, vol. 40, pp. 253–269, 1996.
- [5] —, “Generalization of the theory of signal detectability to  $n$ -event  $m$ -dimensional forced-choice tasks,” *J. Math Psychol.*, vol. 42, pp. 5–31, 1998.
- [6] D. Mossman, “Three-way ROCs,” *Med. Decis. Making*, vol. 19, pp. 78–89, 1999.
- [7] H.-P. Chan, B. Sahiner, L. M. Hadjiiski, N. Petrick, and C. Zhou, “Design of three-class classifiers in computer-aided diagnosis: Monte carlo simulation study,” in Proc. SPIE Vol. 5032 *Medical Imaging 2003: Image Processing*, Milan Sonka and J. Michael Fitzpatrick, Eds., SPIE, Bellingham, WA, 2003, pp. 567–578.
- [8] U. Bick, M. L. Giger, R. A. Schmidt, R. M. Nishikawa, D. E. Wolverton, and K. Doi, “Automated segmentation of digitized mammograms,” *Acad. Radiol.*, vol. 2, pp. 1–9, 1995.

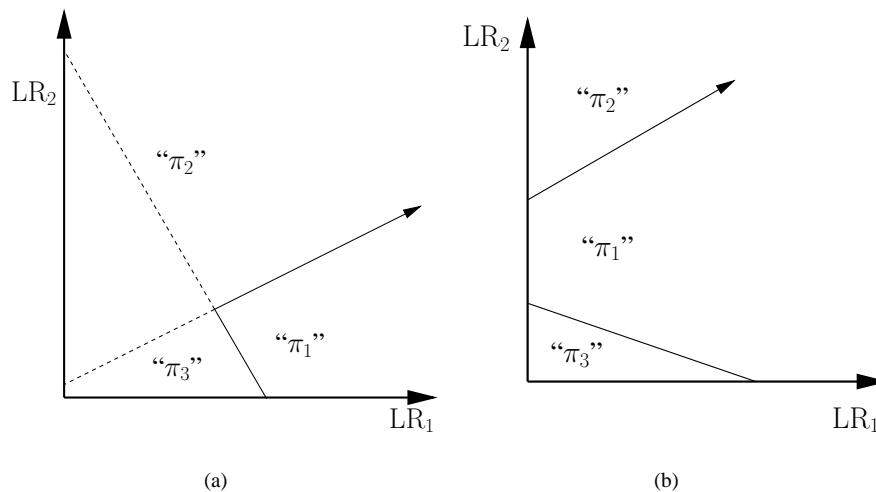


Fig. 14. Example ideal observer decision rules for the case  $\gamma_{313} - \gamma_{323} < 0$  (implying  $1/b_{12} > 0$  and  $1/\chi_{12} < 0$ ) and  $1/b_{13} > 0$ . In (a),  $1/b_{13} < 1/b_{12}$ , and the “2-vs.-3” line can lie anywhere in the unlabeled region; observations above this line will be decided “ $\pi_2$ ”, and those below this line will be decided “ $\pi_3$ ”. In (b),  $1/b_{13} \geq 1/b_{12}$ , and the “2-vs.-3” line can lie anywhere between the “1-vs.-2” and “1-vs.-3” lines (provided it shares their intersection point); note that observations in this region will be decided “ $\pi_1$ ” regardless of the position of this line.

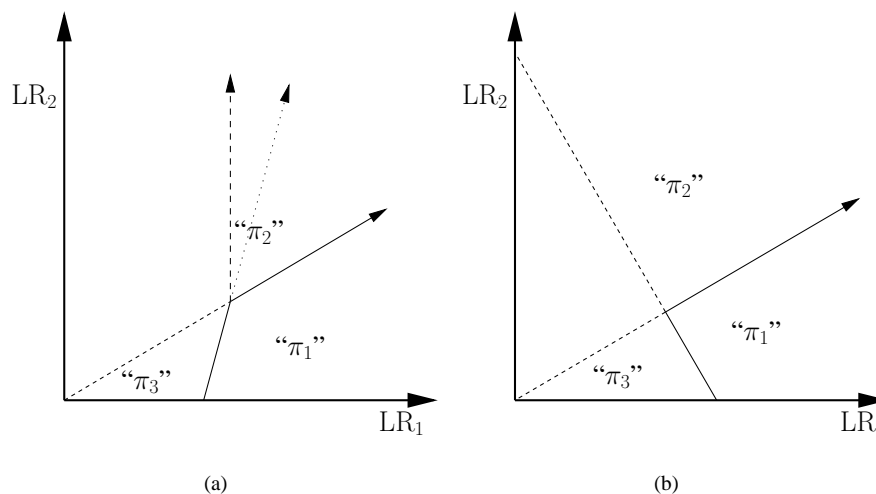


Fig. 15. Example ideal observer decision rules for the case  $\gamma_{313} - \gamma_{323} = 0$  (implying  $1/b_{12} = \mp\infty$  and  $1/\chi_{12} = \pm\infty$ ). In (a),  $1/b_{13} \leq 0$ , and the “2-vs.-3” line can lie anywhere between the two dashed lines shown (the region between the vertical dashed and dotted lines is excluded because  $1/b_{23} \geq 0$ ); observations in the unlabeled region to above this line will be decided “ $\pi_2$ ”, and those below this line will be decided “ $\pi_3$ ”. In (b),  $1/b_{13} > 0$ , and the “2-vs.-3” line can lie anywhere in the unlabeled region; observations above this line will be decided “ $\pi_2$ ”, and those below this line will be decided “ $\pi_3$ ”.

- [9] F.-F. Yin, M. L. Giger, K. Doi, C. E. Metz, C. J. Vyborny, and R. A. Schmidt, “Computerized detection of masses in digital mammograms: Analysis of bilateral subtraction images,” *Med. Phys.*, vol. 18, pp. 955–963, 1991.
- [10] F.-F. Yin, M. L. Giger, C. J. Vyborny, K. Doi, and R. A. Schmidt, “Comparison of bilateral-subtraction and single-image processing techniques in the computerized detection of mammographic masses,” *Invest. Radiol.*, vol. 28, pp. 473–481, 1993.
- [11] F.-F. Yin, M. L. Giger, K. Doi, C. J. Vyborny, and R. A. Schmidt, “Computerized detection of masses in digital mammograms: Automated alignment of breast images and its effect on bilateral-subtraction technique,” *Med. Phys.*, vol. 21, pp. 445–452, 1994.
- [12] M. A. Kupinski, “Computerized pattern classification in medical imaging,” Ph.D. Thesis, The University of Chicago, Chicago, IL, 2000.
- [13] Z. Huo, M. L. Giger, C. J. Vyborny, D. E. Wolverton, R. A. Schmidt, and K. Doi, “Automated computerized classification of malignant and benign masses on digitized mammograms,” *Acad. Radiol.*, vol. 5, pp. 155–168, 1998.
- [14] Z. Huo, M. L. Giger, and C. E. Metz, “Effect of dominant features on neural network performance in the classification of mammographic lesions,” *Phys. Med. Biol.*, vol. 44, pp. 2579–2595, 1999.
- [15] Z. Huo, M. L. Giger, C. J. Vyborny, D. E. Wolverton, and C. E. Metz, “Computerized classification of benign and malignant masses on digitized mammograms: A study of robustness,” *Acad. Radiol.*, vol. 7, pp. 1077–1084, 2000.
- [16] Z. Huo, M. L. Giger, and C. J. Vyborny, “Computerized analysis of multiple-mammographic views: Potential usefulness of special view mammograms in computer-aided diagnosis,” *IEEE Trans. Med. Imag.*, vol. 20, pp. 1285–1292, 2001.
- [17] Z. Huo, M. L. Giger, C. J. Vyborny, and C. E. Metz, “Breast cancer: Effectiveness of computer-aided diagnosis — Observer study with independent database of mammograms,” *Radiology*, vol. 224, pp. 560–568, 2002.
- [18] D. C. Edwards, C. E. Metz, and M. A. Kupinski, “Ideal observers and optimal ROC hypersurfaces in  $N$ -class classification,” *IEEE Trans. Med. Imag.*, vol. 23, pp. 891–895, 2004.
- [19] D. C. Edwards, C. E. Metz, and R. M. Nishikawa, “The hypervolume under the ROC hypersurface of ‘near-guessing’ and ‘near-perfect’ ob-

servers in  $N$ -class classification tasks,” *IEEE Trans. Med. Imag.*, vol. 24, pp. 293–299, 2005.

- [20] A. Srinivasan, “Note on the location of optimal classifiers in  $n$ -dimensional ROC space,” Oxford University Computing Laboratory, Wolfson Building, Parks Road, Oxford, Tech. Rep. PRG-TR-2-99, 1999.
- [21] C. Ferri, J. Hernández-Orallo, and M. A. Salido, “Volume under the roc surface for multi-class problems: Exact computation and evaluation of approximations,” Dep. Sistemes Informàtics i Computació, Univ. Politècnica de València (Spain), Tech. Rep., 2003.
- [22] C. E. Metz, “The optimal decision variable,” unpublished lecture notes for the course “Mathematics for Medical Physicists”, Dept. of Radiology, The University of Chicago, 2000.